Experimental Determination of Chemical Hybridization in Rutile TiO_2 using Site-specific X-ray Photoelectron Spectroscopy

J.C. Woicik[1], E.J. Nelson[1], L. Kronik[2], M. Jain[2], J.R. Chelikowsky[2], D. Heskett[3], L.E. Berman[4], and G.S. Herman[5]

[1]Materials Science and Engineering Laboratory, National Institute of Standards and Technology, Gaithersburg MD

[2]Department of Chemical Engineering and Materials Science, University of Minnesota, Minneapolis, MN

[3]Department of Physics, University of Rhode Island, Kingston, RI

[4]National Synchrotron Light Source, Brookhaven National Laboratory, Upton, NY

[5]Hewlett-Packard Company, Corvallis, OR

X-ray photoelectron spectroscopy (XPS) has emerged as a premier method by which to study the chemical bonding in solids. Owing to the conservation of energy between the incident photon and the ejected photoelectron, XPS has provided much direct and important information pertaining to the occupied electronic density of states for many materials. However, because XPS measures the transition probabilities between the initial, bound-state valence electrons and the final, plane-wave continuum-state photoelectrons, the technique does not render the density of occupied electronic states. Rather, it produces the density of these states modulated by the electronic transition-probability matrix elements.

As these transitions conserve orbital angular momentum, the XPS valence photocurrent resulting from a crystal-valence band may be written within a one-electron approximation as

$$I(E,h\nu) \propto \Sigma_{i,l}\, \rho_{i,l}(E)\, \sigma_{i,l}(E,h\nu). \qquad (1)$$

Here E is the photoelectron binding energy, $h\nu$ is the x-ray photon energy, $\rho_{i,l}(E)$ are individual, angular-momentum l resolved, electronic single-particle partial density of states of the i^{th} atom of the crystalline-unit cell, and $\sigma_{i,l}(E,h\nu)$ are the angle-integrated, angular-momentum dependent, photoionization cross sections. Despite the general acceptance of Eqn. (1), the different weights of the angular-momentum components of the crystalline electronic structure are only seldom considered in the interpretation of photoelectron spectra.

Here, we employ the newly developed technique of site-specific x-ray photoelectron spectroscopy [1] that utilizes the sinusoidal spatial dependence of the electric-field intensity near a crystal x-ray Bragg reflection to *experimentally* determine chemical hybridization in rutile TiO_2 by measuring the individual Ti and O contributions to the valence band. Comparisons with state-of-the art, *ab initio* local density approximation (LDA) calculations of the Ti and O partial density of states demonstrate the importance of the individual angular-momentum components of the crystal-valence band and their direct relevance to the solid-state electronic structure. This analysis facilitates a proper interpretation of the electronic structure of rutile TiO_2 by photoelectron spectroscopy, which should serve as a benchmark for the interpretation of the more complex transition-metal oxides (TMO's) and the unique physical phenomena, such as Mott transitions, colossal magnetoresistance, and high-temperature superconductivity, that they exhibit.

The experiment was performed at the National Institute of Standards and Technology beamline X24A at the NSLS. The double-crystal monochromator was operated with Si(111) crystals, and high-resolution photoelectron spectra were obtained with a hemispherical electron analyzer. Atomically clean, stochiometric single-crystal rutile TiO_2(110) surfaces were prepared by 500 eV Ar sputtering followed by annealing in 7 x 10^{-7} torr of O_2 at 650° C. This procedure produced sharp (1x1) low-energy electron diffraction patterns and a crystal that was slightly reduced showing no signs of charging from exposure to the x-ray beam.

The photoelectron spectra are shown in Figure 1. They have been recorded at two different photon energies within the photon-energy width ($\Delta E \sim 0.38$ eV) of the rutile TiO_2(200) Bragg back-reflection condition ($h\nu \sim 2700$ eV) that were chosen to maximize the electric-field intensity on either the Ti or O atomic planes. The spectra extend over the kinetic-energy range of the Ti

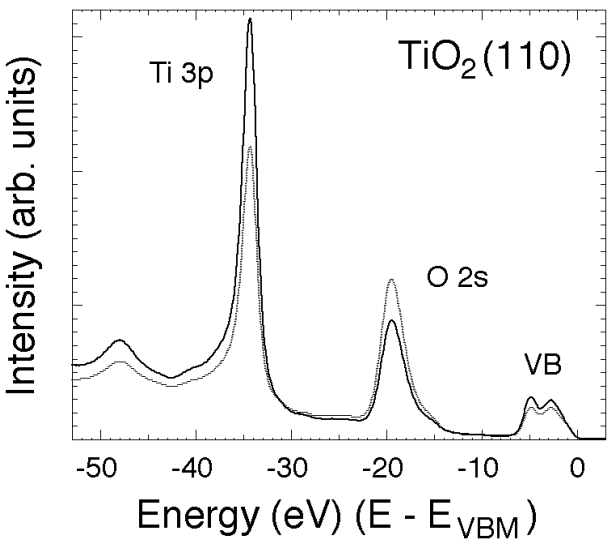

Figure 1. *Photoelectron spectra from the rutile TiO_2(110) surface recorded within the photon-energy width of the TiO_2(200) Bragg back-reflection condition. The spectra have been referenced to the valence-band maximum and extend over the kinetic-energy range of the Ti 3p, O 2s, and valence-electron emission. The photon energies were chosen to maximize the electric-field intensity on either the Ti (bold line) or O (shaded line) atomic planes. Note the enhancement of the emission from either the Ti or O atoms depending on which set of atomic planes was preferentially excited.*

3p and O 2s core lines, as well as the crystal-valence band. The well-known x-ray standing-wave effect [2] is observed for each of the core lines, as well as for the crystal-valence band [1].

Before we address the individual electronic partial density of states, it is useful to examine the valence-photoelectron spectrum recorded off of the Bragg condition ($h\nu$ ~ 2695 eV). Away from the Bragg condition, the electric-field intensity is constant over the dimensions of the crystalline-unit cell, and the resulting spectrum is representative of the total rutile electronic structure. This spectrum is shown in Figure 2. It is compared to an *ab initio* LDA calculation of the total electronic density of states. (The curve labeled "c-theory" is addressed below.) The curves have been scaled to equal peak height and referenced to the valence-band maximum that was determined for the experimental spectrum by extrapolating the straight portion of the maximum of negative slope to zero electron emission. The theoretical calculation was convolved with a Gaussian of width 0.4 eV to simulate the total experimental resolution.

The calculations were performed by using *ab initio* Troullier-Martins pseudopotentials within the local density approximation using a plane-wave basis [3]. Pseudopotentials based on electronic configurations of $3s^2 3p^6 4s^0 3d^2$ (Ti) and $2s^2 2p^4$ (O) were used, with s/p/d (Ti) and s/p (O) cutoff radii (in atomic units) of 2.3/1.5/2.25 and 1.45/1.45, respectively. A plane-wave cutoff energy of 120 Ry and a 4x4x6 Monkhorst-Pack k-point sampling scheme were used to guarantee convergence. We obtained values of a = 4.57 Å, c/a = 0.643, and u=0.303 for the structural parameters of the rutile TiO_2 phase. These values are in excellent agreement with the experimental values of a = 4.59 Å, c/a = 0.644, and u = 0.305 [4].

At first glance, the LDA calculation may seem to reproduce adequately the experimental photoemission density of states curve; however, this agreement is fortuitous. In fact, careful inspection of the data and calculation reveals a poor energy alignment and a poor agreement on the widths of the two lobes characteristic of the rutile photoelectron spectrum. Note as well that the second lobe in the experimental photoemission spectrum actually occurs at the energy position of the shoulder to the second lobe produced by the theory.

In order to establish the origins of these discrepancies, the individual Ti and O components of the rutile valence band were computed from the spectra of Figure 1. The spectra were aligned relative to the energy position of the Ti 3p core line, and normalized to the electric-field intensities at the Ti and O core sites that were taken as the areas of the Ti 3p and O 2s core lines. After removing an integrated background from

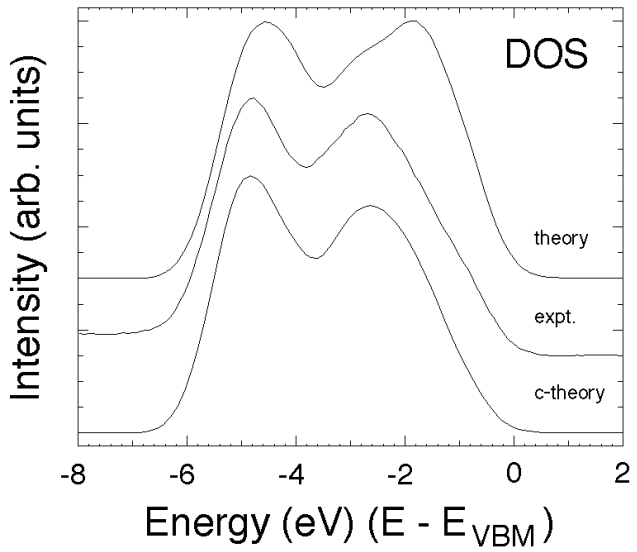

Figure 2. *Comparison of the theoretical total electronic density of states (upper), the valence-photoelectron spectrum recorded off of the Bragg condition (middle), and the theoretical total electronic density of states corrected for individual Ti and O angular-momentum dependent photoelectron cross sections (lower). The curves have been scaled to equal peak height.*

the valence-band region, linear combinations of the two spectra yielded the *experimental* photoemission partial density of states curves around the Ti and O sites, as shown in Figure 3. Clearly, the large contribution of Ti to the valence-band spectrum indicates significant covalent bonding between the Ti and O atoms, despite the formal Ti^{4+} charge state of Ti in rutile. Had Ti been completely ionized, there would be no Ti valence-electron emission.

In order to understand the implications of these findings and to further test the validity of the LDA approximation, theoretical Ti and O partial density of states curves, also shown in Figure 3, were computed by deconvolving the obtained wave functions over atomic orbitals of valence electrons. Spheres of ~ 1.3 Å and ~ 0.75 Å for Ti and O, respectively, centered around each atom, were used for the deconvolution. These sphere radii are close to the covalent radii of the atomic species involved. The resulting partial densities of states were only weakly dependent on the radius chosen, within a range of ± 0.2 Å around this radius.

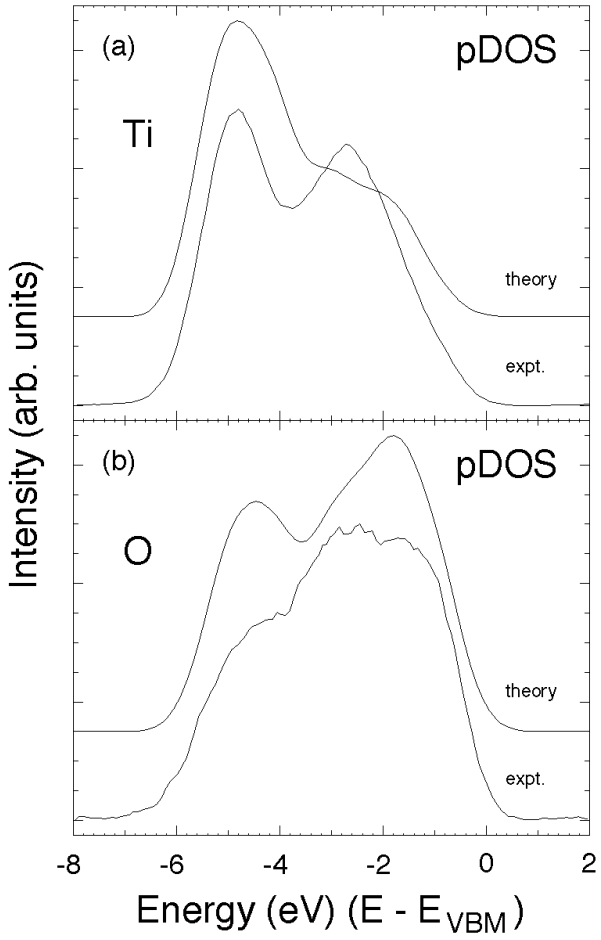

Figure 3. *Comparison of the theoretical partial density of states with the experimental valence-photoelectron spectrum. a) Ti. b) O. Theoretical and experimental curves have been scaled to equal peak height. The O component has been scaled by a factor of 4 relative to the Ti component.*

Clearly, agreement between theory and experiment is much less than satisfactory, and it is significantly worse than had been suggested by Figure 2. In particular, the second lobe of the Ti valence band is nearly absent in the theory, and the triply peaked structure of the O valence band is poorly reproduced. Furthermore, it is clear that no weighted linear combination of the theoretical Ti and O partial density of states, attempting to account for the different photoelectron cross sections of the Ti 3d and O 2p orbitals, would produce a more accurate representation of the experimental data.

For this reason, the theoretical Ti and O partial density of states were decomposed into their angular-momentum resolved components. These curves are shown in Figure 4. From inspection of these curves, it is clear that the second lobe of the experimental Ti spectrum cannot be reproduced without inclusion of the Ti 4p component, and the intermediate structure of the experimental O spectrum cannot be reproduced without inclusion of the O 2s component.

Drawing on the physical insight gleaned from Eqn. (1), we re-calculated the partial density of states curves from the weighted sums of the different orbital components of Figure 4 using the tabulated theoretical atomic cross sections (Ti σ_{4s}/σ_{3d} ~ 9.9 and O σ_{2s}/σ_{2p} ~ 29) [5]. Agreement between the theoretical and experimental partial density of states was much improved; however, even better agreement was obtained for both the Ti and O components if the relative atomic cross sections were scaled by an additional factor of 2. We note that up to 1.5 of this factor of 2 could come from the choice of convolution radius, in addition to changes in the atomic cross sections in the solid state. The resulting theoretical *corrected* partial density of states is shown in Figure 5, together with the experimental data. The agreement now between theory and experiment is startling. We note that this agreement has been achieved without any energy dependence of the cross sections across the energy width of the valence band or the consideration of many-body effects. Additionally, it is clear that orbitals with smaller values of *l* are emphasized in the photoemission process.

We may now re-calculate the total density of states from the theoretical corrected Ti and O partial density of states using the *experimental* Ti and O *total* cross sections determined from the areas of the individual Ti and O components of the rutile valence band (Ti_{VB}/O_{VB} ~ 3.4). Figure 2 compares the resulting theoretical corrected total density of states with the photoelectron spectrum recorded off of the Bragg condition. Clearly, the agreement between theory and experiment is no longer fortuitous.

At this point, it is instructive to consider the molecular orbitals for an octahedral complex containing a first-row transition-metal ion [6]. This model of the electronic structure of the TMO's is based on the chemical bonding between the metal 3d, 4s, and 4p states, and the ligand 2s and 2p states within octahedral (O_h) symmetry, although the octahedral environment around the cation is usually slightly distorted. In this depiction, the metal 4s orbitals bond with the ligand s orbitals to form the $a_{1g}(\sigma^b)$ level, the metal $3d_{x2-y2}$ and $3d_{z2}$ orbitals bond with the ligand s orbitals to form the $e_g(\sigma^b)$ level, the metal 4p orbitals bond with both the ligand σ and π orbitals to form the $t_{1u}(\sigma^b)$ and $t_{1u}(\pi^b)$ levels, and the metal $3d_{xy}$, $3d_{xz}$, and $3d_{yz}$ orbitals bond with the ligand π orbitals to form the $t_{2g}(\pi^b)$ level. Additionally, there are ligand p orbitals ($t_{1g}(\pi)$ and $t_{2u}(\pi)$) that are left over and are rigorously non-bonding in O_h symmetry.

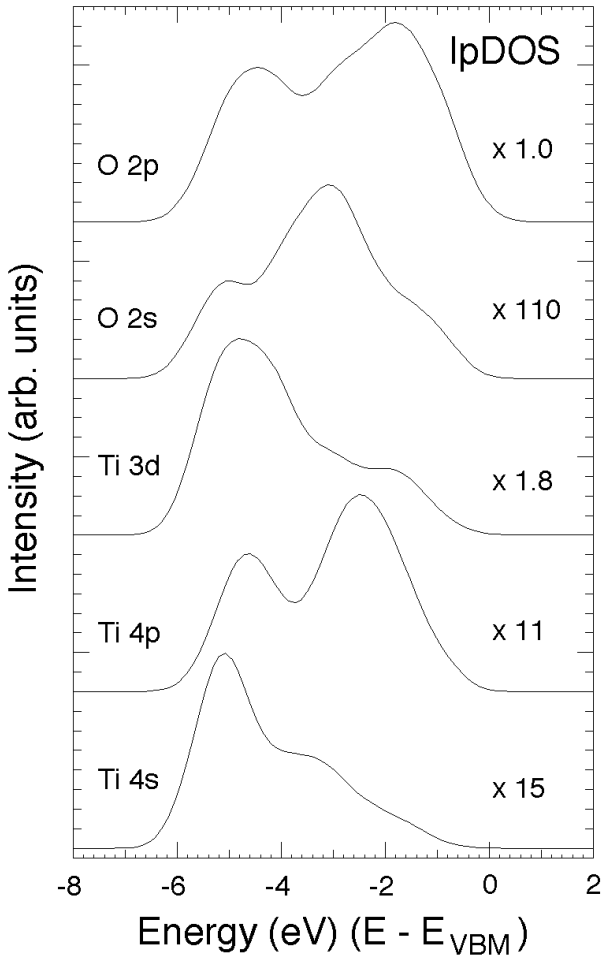

Figure 4. *Comparison of the different* angular-momentum *components of the theoretical Ti and O partial density of states. Multipliers relative to the O 2p component are indicated in each case.*

Examination of both the experimental partial density of states and the theoretical corrected partial density of states of Figure 5 leads to an attractive interpretation of the electronic structure within this s and p bonding scheme. The doubly lobed Ti structure of the valence band may be attributed to the energy splitting between the σ and π groupings of the bonding states, with the σ bonds lying at the lower energy due to the increased overlap of the σ bonds relative to the π bonds. These states are mirrored in the triply lobed O structure, and they occur at the same energy as in the Ti spectrum indicating the sharing of electrons in a covalent bond. The O non-bonding π states then naturally compose the third lobe of the O spectrum; they occur at higher energy than the O bonding π states and reveal little or no electron density on the metal atoms, as expected. Close inspection of the angular-momentum resolved components of Figure 4 supports these conclusions, although the solid-state electronic structure is much more complicated than the electronic structure of an octahedral TiO_6 molecule. In particular, the groupings of the orbitals into discrete σ and π states are not as transparent, and the effect of translational symmetry spreads the states into bands (Bloch functions). Additionally, metal-metal and ligand-ligand interactions that are not present in isolated molecules are known to affect the valence electronic structure significantly.

Despite the apparent shortcomings of the molecular orbital theory, it is instructive to examine the hybridization of the metal and ligand orbitals within this bonding scheme. As both the O 2s and $2p_z$ atomic orbitals belong to the same symmetry representation of the O_h point group, the ligand s orbitals, $| \psi_{L,\sigma} >$, will contain a mixture of these states; i.e., $| \psi_{L,\sigma} > = \alpha | 2s > + \sqrt{(1 - \alpha^2)} | 2p_z >$. (The ligand π orbitals are constructed solely from the O $2p_x$ and $2p_y$ atomic orbitals.) This hybridization orients the ligand-charge density towards the metal atoms, leading to an increased overlap between the metal and ligand wave functions. It has been stated by Mulliken that "a little bit of hybridization goes a long way" to stabilize a chemical bond, and, from the theoretical calculations of Figure 4, we see that α, the mixing coefficient, is only ~ 10 %, even though the O 2s valence component accounts for as much as ~ 30 % of the experimental O valence spectrum (due to the much larger cross section of the O 2s orbitals versus the O 2p ones).

This relatively small value of α results from the relatively large energy separation between the O 2s and 2p atomic orbitals that, as seen from the data in Figure 1, is ~ 17 eV, while the hybrid energy of the combined O 2s and 2p orbitals occurs near the top of the valence band, i.e., much closer to the energy of the O 2p atomic orbitals. On the other hand, the energy separation be-

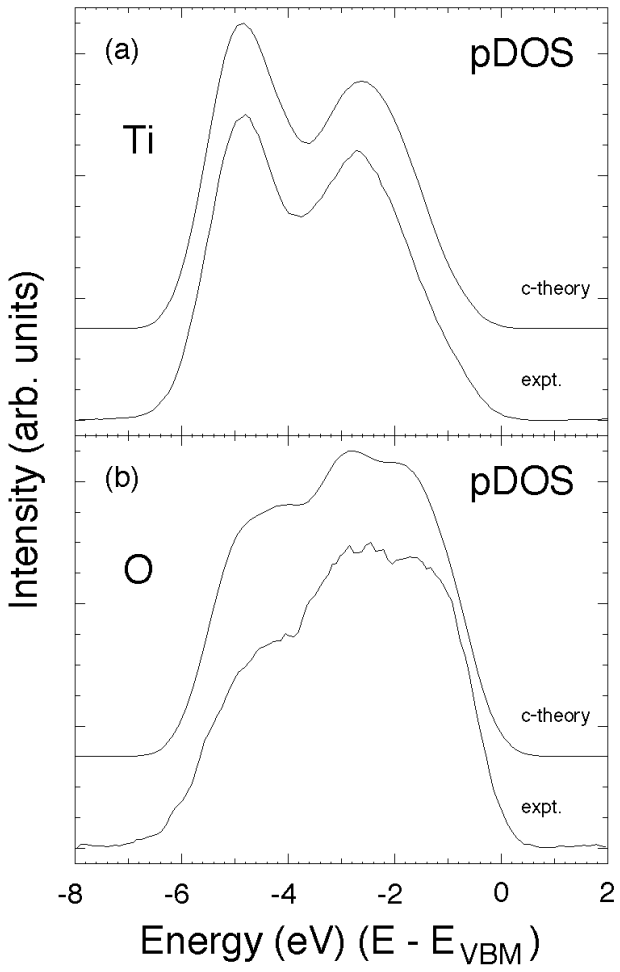

Figure 5. *Comparison of the theoretical partial density of states, corrected for individual angular-momentum dependent photoelectron cross sections, with the experimental valence-photoelectron spectrum. a) Ti. b) O. The curves have been scaled to equal peak height.*

tween the Ti 3d, 4s, and 4p atomic orbitals is significantly less (~ 8 eV) [6,7], accounting for the much larger amount of Ti 3d, 4s, and 4p hybridization observed on the Ti sites. Amusingly, it is the added complexity of the photoemission process, i.e., the "over-representation" of some orbitals due to the angular-momentum dependence of the atomic cross sections, that affords this direct experimental observation of chemical hybridization in the solid-state electronic structure, that is, the observation of σ and π bonds and of oxygen non-bonding states, and the positive identification of valence-band contributions from the O 2s and the Ti 4s and 4p orbitals.

Acknowledgements

This work was performed at the National Synchrotron Light Source, Brookhaven National Laboratory, which is supported by the U.S. Department of Energy, Division of Materials Sciences and Division of Chemical Sciences, under Contract No. DE-AC02-98CH10886. Additional support was provided by the National Institute of Standards and Technology, the National Science Foundation, the Computational Materials Science Network of the Department of Energy, and the Minnesota Supercomputing Institute.

References

[1] J.C. Woicik, E.J. Nelson, and P. Pianetta, "Direct measurement of valence-charge asymmetry by x-ray standing waves," Phys. Rev. Lett., 84, *773*, 2000; J.C. Woicik, E.J. Nelson, T. Kendelewicz, P. Pianetta, M. Jain, L. Kronik, and J.R. Chelikowsky, "Partial density of occupied valence states by x-ray standing waves and high-resolution photoelectron spectroscopy," Phys. Rev. B, 63, *R41403*, 2001; J.C. Woicik, E.J. Nelson, D. Heskett, J. Warner, L.E. Berman, B.A. Karlin, I.A. Vartanyants, M.Z. Hasan, T. Kendelewicz, Z.X. Shen, and P. Pianetta, "X-ray standing wave investigations of valence electronic structure," Phys. Rev. B, 64, *125115*, 2001.

[2] J. Zegenhagen, "Surface structural determination with x-ray standing waves," Surf. Sci. Rep., **18**, *199*, 1993.

[3] K.M. Glassford and J.R. Chelikowsky, "Structural and electronic properties of titanium dioxide," Phys. Rev. B, 46, *1284*, 1992.

[4] S. C. Abrahams and J. L. Bernstein, "Rutile: Normal probability plot analysis and accurate measurement of crystal structure," J. Chem. Phys., **55**, *3206*, 1971.

[5] M.B. Trzhaskovskaya, V.I. Nefedov, and V.G. Yarzhemsky, "Photoelectron angular distribution parameters for elements z = 1 to z = 54 in the photoelectron energy range 100 - 5000 eV," Atomic Data and Nuclear Tables, 77, *97*, 2001. Unfortunately, the Ti 4p atomic cross section is not tabulated; consequently, we took it to be equal to the Ti 4s one.

[6] C.J. Ballhausen and H.B. Gray, *Molecular Orbital Theory* (Benjamin, New York, 1964), Chaps. 4 and 8. As in the text, we adopt a coordinate system on each ligand that directs the ligand z axis towards the metal ion.

[7] Z. Zhang, S.-P. Jeng, and V.E. Henrich, "Cation-ligand hybridization for stoichiometric and reduced TiO_2(110) surfaces determined by resonant photoemission," Phys. Rev. B, 43, *12004*, 1991.